Article

Protein and Electrode Engineering for the Covalent Immobilization of P450 BMP on Gold

Valentina E. V. Ferrero, Laura Andolfi, Giovanna Di Nardo, Sheila J. Sadeghi, Andrea Fantuzzi, Salvatore Cannistraro, and Gianfranco Gilardi

Anal. Chem., **2008**, 80 (22), 8438-8446 • DOI: 10.1021/ac8011413 • Publication Date (Web): 24 October 2008

Anal. Chem. **2008,** *80,* 8438–8446

Protein and Electrode Engineering for the Covalent Immobilization of P450 BMP on Gold

Valentina E. V. Ferrero,[†] Laura Andolfi,[‡] Giovanna Di Nardo,[†] Sheila J. Sadeghi,[†] Andrea Fantuzzi,[§] Salvatore Cannistraro,*[,‡] and Gianfranco Gilardi*[,†,§]

Division of Molecular Biosciences, Biochemistry Building, Imperial College London, SW7 2AZ, London, United Kingdom, Biophysics and Nanoscience Centre, CNISM, Facoltà di Scienze, Università della Tuscia, 01100, Viterbo, Italy, and Department of Human and Animal Biology, University of Torino, 10123, Torino, Italy

Site-directed mutagenesis and functionalization of gold surfaces have been combined to obtain a stable immobilization of the heme domain of cytochrome P450 BM3 from *Bacillus megaterium*. Immobilization experiments were carried out using the wild type protein bearing the surface C62 and C156 and the site-directed mutants C62S, the C156S, and the double mutant C62S/C156S (no exposed cysteines). The gold surface was functionalized using two different spacers: cystamine-*N*-succinimidyl 3-maleimidopropionate and dithio-bismaleimidoethane, both leading to the formation of maleimide-terminated monolayers capable of covalent linkage to cysteine. Tapping mode atomic force microscopy experiments carried out on cystamine-*N*-succinimidyl 3-maleimidopropionate derivatized gold led to good images with expected molecular heights (5.5−6.0 nm) for the wild type and the C156S mutant. These samples also gave measurable electrochemical signals with midpoint potentials of −48 and −58 mV for the wild type and C156S, respectively. On the other hand, the dithio-bismaleimidoethane spacer led to variability on the molecular heights measured by tapping mode atomic force microscopy and the electrochemical response. This is interpreted in terms of lack of homogeneous dithio-bismaleimidoethane monolayer on gold. Furthermore, results from tapping mode atomic force microscopy show that the double mutant and the C62S did not lead to stably immobilized P450 protein, confirming the necessity of the solvent exposed C62.

In recent years much work has been dedicated to the integration of redox proteins and enzymes with electronic transducers.[1−3] In particular, cytochromes P450 (P450s) are heme thiolate proteins present in most organisms where they play a crucial role in the metabolism of both endogenous and foreign compounds. They are able to catalyze a wide range of reactions such as hydroxylations, epoxidations or N- and O-dealkylations[4] by using two electrons, provided by a NAD(P)H-dependent reductase, dioxygen and two protons.

Cytochrome P450-BM3 (CYP102A1) from *Bacillus megaterium* is a catalitically self-sufficient monooxygenase with a P450 heme domain (BMP) fused via a peptide linker to the reductase domain in a single polypeptide chain of 119 kDa.[5] The X-ray structure of BMP shows that this domain bears three cysteines: C62 and C156 that are solvent exposed and Cys 400 that is engaged as the heme ligand.[6,7]

P450 BM3 is able to recognize a broad range of substrates, including alcohols, fatty acids, alkanes, amides, hydrocarbons, and polyaromatic hydrocarbons, heterocycles.[8] It has been also found that it is able to turn over compounds normally metabolized by human CYP3A4, CYP2E1, and CYP1A2.[9]

Over the years, much attention has been dedicated to these enzymes for the development of bioelectrodes both for analytical[10] and bioelectrocatalytic purposes[11] as well as for bioremediation,[12] biotransformation,[13] and production of drugs and their metabolites.[14−16]

* To whom correspondence should be addressed. G. Gilardi, Division of Molecular Biosciences, Imperial College London, London SW7 2AZ. U.K. Phone: (+) 44 207 5945320. Fax: (+) 44 207 5945330. E-mail: g.gilardi@imperial.ac.uk. S. Cannistraro, Department of Environmental Science, University of Tuscia, 01100, Viterbo, Italy. E-mail: salvatore.cannistraro@unitus.it.

[†] University of Torino.

[‡] Università della Tuscia.

[§] Imperial College London.

(1) Willner, B.; Katza, E.; Willner, I. *Curr. Opin. Biotechnol.* **2006**, *17* (6), 589–596.

(2) Bonanni, B.;Alliata, D.;Andolfi, L.;Bizzarri, A.R.;Cannistraro, S. *Surface Science Research Developments;* Norris, C. P., Ed.; Nova Science Publishers: Hauppauge, NY,2005; pp 1−73.

(3) Gilardi, G.; Fantuzzi, A.; Sadeghi, S. *Curr. Opin. Struct. Biol.* **2001**, *11* (4), 491–499.

(4) Montellano, P. R. O. *Cytochrome P450: Structure, Mechanism and Biochemistry*, 3rd ed.; Plenum Publishers: New York, 2005.

(5) Narhi, L. O.; Fulco, A. J. *J. Biol. Chem.* **1986**, *261* (16), 7160–7169.

(6) Sevrioukova, I. F.; Li, H.; Zhang, H.; Peterson, J. A.; Poulos, T. L. *Proc. Natl. Acad. Sci. U.S.A.* **1999**, *96* (5), 1863–1868.

(7) Sevrioukova, I. F.; Hazzard, J. T.; Tollin, G.; Poulos, T. L. *J. Biol. Chem.* **1999**, *274* (51), 3609739106(b)

(8) Munro, A. W.; Leys, D. G.; McLean, K. J.; Marshall, K. R.; Ost, T. W. B.; Daff, S.; Miles, C. S.; Chapman, S. K.; Lysek, D. A.; Moser, C. C.; Page, C. C.; Dutton, P. L. *Trends Biochem. Sci.* **2002**, *27*, 250–257.

(9) Di Nardo, G.; Fantuzzi, A.; Sideri, A.; Panicco, P.; Sassone, C.; Giunta, C.; Gilardi, G. *J. Biol. Inorg. Chem.* **2007**, *12* (3), 313–323.

(10) Bistolas, N.; Wollenberger, U.; Jung, C.; Scheller, F. W. *Biosens. Bioelectron.* **2005**, *20*, 2408–2423.

(11) Udit, A. K.; Hill, M. G.; Gray, H. B. *Langmuir* **2006**, *22* (25), 10854–10857.

(12) Blair, E.; Greaves, J.; Farmer, P. J. *J. Am. Chem. Soc.* **2004**, *126* (28), 8632–8633.

(13) De Mot, R.; Parret, A. H. A. *Trends Microbiol.* **2002**, *10* (11), 502–508.

(14) Guengerich, F. P. *Biol. Chem.* **2002**, *383* (10), 1553–1564.

(15) Otey, C. R.; Bandara, G.; Lalonde, J.; Takahashi, K.; Arnold, F. H. *Biotechnol. Bioeng.* **2006**, *93* (3), 494–499.

(16) Kanayama, N.; Kanari, C.; Masuda, Y.; Ohmori, S.; Ooie, T. *Xenobiotica* **2007**, *37* (2), 139–154.

10.1021/ac8011413 CCC: $40.75
Published on Web 10/24/2008

Relevant to these studies, BMP can use an electrode as an electron source.[17,18]

Sensitivity and specificity are of fundamental importance when designing a biosensor, it is recognized that these parameters are strongly affected by the strategies adopted during the immobilization of the enzyme. The surface concentration and the orientation of the enzyme on the electrode, the distance between the redox center and the surface,[19] the choice of electrode material, and the presence of anchoring spacers all contribute to preserve the unaltered biological functionality of the immobilized protein.[11,20,21] The protein can be linked to the surface thanks to physical, electrostatic, hydrophobic, or covalent interactions depending on its own properties or to the surface features.[22,23] The role of protein orientation in electron transfer to the electrode has also been addressed by utilization of different binding groups on the opposite sides of the same protein.[24−27]

Ionic surfactants such as a dimethyldidodecylammonium bromide and poly(dimethylallylammonium bromide) have been used to noncovalently immobilize cytochrome P450s on the surface of glassy carbon and gold electrodes.[11,17,18,20,28]

On the other hand, covalent linkage of the protein to gold, with or without the use of self-assembled monolayers, gives the advantage of obtaining a stable and oriented immobilization of the biomolecule. In such a case the thiol group of unique cysteine residue on the protein surface can be exploited to covalently link to Au atoms.[29,30] The position of cysteine residues can be suitably modulated by site-directed mutagenesis, and this has been obtained for some redox proteins such as azurin,[2,31] plastocyanin,[32,33] yeast cytochrome c,[34,35] and for cytochrome P450cam.[36]

However, direct linkage of the protein on metal surfaces may cause a partial denaturation and the loss of activity.[37,38] In this case several flexible spacer molecules can be used as self-assembling monolayers on gold exposing thiol reactive groups such as maleimide, thiol, and disulfide groups able to mask the metal surface and, at the same time, provide an anchor to the protein.[28,39−42]

In recent years, among other techniques, tapping mode atomic force microscopy (TMAFM) has become a powerful method for investigating the way in which proteins assemble on a surface. This technique enables one to visualize single biological molecules in fluid with a minimal mechanical perturbation of the sample. As a result, the analysis of the molecular height as obtained by TMAFM can provide important indication about structural stability and orientation of the immobilized protein.

In this work, site-directed mutagenesis and gold surface functionalization have been combined to obtain a stable BMP immobilization on gold electrode. Site-directed mutagenesis has been applied to selectively replace one by one the cysteine residues on BMP with serines, thus creating two mutants, C156S and C62S exposing either C62 or C156. These mutants were used to assess the importance of unique anchoring points for binding to either a bare or functionalized gold substrate surface. A double mutant (C62S/C156S), with both cysteines substituted by serines, was also created as a negative control.

The gold surface functionalization has been achieved by using two different spacers, cystamine-*N*-succinimidyl 3-maleimidopropionate (CST-MALM) and dithio-bismaleimidoethane (DTME), that lead to the formation of maleimide-terminated monolayers. These two spacers were chosen not only because they adopt two different strategies for the formation of the self-assembled monolayers but also because of the different length of the final spacer molecule.

The two chemical approaches exploited to attain the specific attachment of wild type and single BMP mutants onto bare and functionalized gold surface have been investigated at single molecule level by high resolution TMAFM. Findings from such studies are aimed at shedding light on the best strategy for covalent attachment of cytochrome P450 BMP biomolecules on gold electrode for future design of potentially useful P450 sensing devices.

MATERIALS AND METHODS

Site Directed Mutagenesis, Expression and Purification of Wild Type, C62S, C156S, C62S/C165S BMP. Surface exposed cysteines were removed by site-directed mutagenesis in the BMP gene present in the T7 plasmid.[43] Site-directed mutagenesis was carried out using the QuikChange kit (Stratagene,

(17) Fleming, B. D.; Tian, Y.; Bell, S. G.; Wong, L. L.; Urlacher, V.; Hill, H. A. *Eur. J. Biochem.* **2003**, *270* (20), 4082–4088.
(18) Fantuzzi, A.; Meharenna, Y. T.; Briscoe, P. B.; Sassone, C.; Borgia, B.; Gilardi, G. *Chem. Commun.* **2006**, *12*, 1289–1291.
(19) Marcus, R. A.; Sutin, N. *Biochim. Biophys. Acta* **1985**, *811* (33), 265–332.
(20) Gilardi, G.; Fantuzzi, A. *Trends Biotechnol.* **2001**, *19* (11), 468–476.
(21) Katz, E.; Willner, I. *Electroanalysis* **2003**, *15* (11), 913–947.
(22) Williams, D. E.; Armstrong, F. A.; Barnett, C. J.; Calvo, E. J.; Amatore, C.; Wilson, G. S.; Oldfield; Parsons; Cass, A. E. G.; Gilardi, G.; Canters, G. W.; Magner; Rivera, M.; Rusling, J. F.; Schiffrin, D. J.; Pickett, C. J.; Willner, I.; Heller, A.; Schuhmann, W.; Gorton, L.; Magner *Faraday Discuss.* **2000**, *116*, 257–268.
(23) Rusling, J. F. *Acc. Chem. Res.* **1998**, *31* (6), 363–369.
(24) Trammell, S. A.; Wang, L.; Zullo, J. M.; Shashidhar, R.; Lebedev, N. *Biosens. Bioelectron.* **2004**, *19* (12), 1649–1655.
(25) Trammell, S. A.; Spano, A.; Price, R.; Lebedev, N. *Biosens. Bioelectron.* **2006**, *21* (7), 1023–1028.
(26) Lebedev, N.; Trammell, S. A.; Spano, A.; Lukashev, E.; Griva, I.; Schnur, J. *J. Am. Chem. Soc.* **2006**, *128* (37), 12044–12045.
(27) Trammell, S. A.; Griva, I.; Spano, A.; Tsoi, S.; Tender, L. M.; Schnur, J.; Lebedev, N. *J. Phys. Chem. C* **2007**, *111* (45), 17122–17130.
(28) Fantuzzi, A.; Fairhead, M.; Gilardi, G. *J. Am. Chem. Soc.* **2004**, *126* (16), 5040–5041.
(29) Ulman, A. *Chem. Rev.* **1996**, *96* (4), 1533–1554.
(30) Bizzarri, A. R.; Bonanni, B.; Costantini, G.; Cannistraro, S. *ChemPhysChem* **2003**, *4* (11), 1189–1195.
(31) Chi, Q. J.; Zhang, J. D.; Nielsen, J. U.; Friis, E. P.; Chorkendorff, I.; Canters, G. W.; Andersen, J. E. T.; Ulstrup, J. *J. Am. Chem. Soc.* **2000**, *122* (17), 4047–4055.
(32) Andolfi, L.; Cannistraro, S.; Canters, G. W.; Facci, P.; Ficca, A. G.; Van Amsterdam, I. M. C.; Verbeet, M. P. *Arch. Biochem. Biophys.* **2002**, *399* (1), 81–88.
(33) Andolfi, L.; Bonanni, B.; Canters, G. W.; Verbeet, M. P.; Cannistraro, S. *Surf. Sci.* **2003**, *530* (3), 181–194.
(34) Bonanni, B.; Alliata, D.; Bizzarri, A. R.; Cannistraro, S. *ChemPhysChem.* **2003**, *4* (11), 1183–1188.
(35) Heering, H. A.; Wiertz, F. G. M.; Dekker, C.; de Vries, S. *J. Am. Chem. Soc.* **2004**, *126* (35), 11103–11112.
(36) Davis, J. J.; Djuricic, D.; Lo, K. K. W.; Wallace, E. N. K.; Wong, L. L.; Hill, H. A. O. *Faraday Discuss.* **2000**, *116*, 15–22.
(37) Armstrong, F. A. *Struct. Bond.* **1990**, *72*, 137–221.
(38) Zhou, Y. X.; Nagaoka, T.; Zhu, G. Y. *Biophys. Chem.* **1999**, *79* (1), 55–62.
(39) Smith, E. A.; Wanat, M. J.; Cheng, Y.; Barreira, S. V. P.; Frutos, A. G.; Corn, R. M. *Langmuir* **2001**, *17* (8), 2502–2507.
(40) Wegner, G. J.; Lee, N. J.; Marriott, G.; Corn, R. M. *Anal. Chem.* **2003**, *75* (18), 4740–4746.
(41) Andolfi, L.; Bizzarri, A. R.; Cannistraro, S. *Thin Solid Films* **2006**, *515* (1), 212–219.
(42) Delfino, I.; Bonanni, B.; Andolfi, L.; Baldacchini, C.; Bizzarri, A. R.; Cannistraro, S *J. Phys.: Condens. Matter* **2007**, *19* (22), 1–18.
(43) Darwish, K; Li, H. Y.; Poulos, T. L. *Protein Eng.* **1991**, *4* (6), 701–708.

CA) using the following two primers for C62S and C156S mutations (serine residue is underlined): (1) C62S, 5′ TAAAGAAGCAAGTGATGAATCACGC 3′; (2) C156S, 5′ TTGGTCTTTCGGGCTTTAACTATCG 3′. The mutations introduced were verified by DNA sequencing.

Freshly transformed *Escherichia coli* BL21 (DE3) cells (either with pT7BMPwt or the mutants) were grown in LB media with ampicillin (100 μg/mL) and induced with IPTG 1 mM. After induction, the cells were allowed to grow for a further 18 h at 28 °C. The protein was isolated and purified following previously published procedures.[44]

The functionality of purified BMP was verified spectrophotometrically. The protein was reduced by the addition of small amounts of dithionite (DT) and its spectrum recorded. Carbon monoxide (CO) was bubbled into the latter protein solution for a few minutes, and the resulting spectrum was recorded. Upon binding of CO to the reduced form of the protein, the characteristic 450 nm absorbance peak was observed. Enzyme concentrations were calculated using an extinction coefficient of 91 000 cm^{-1} M^{-1} at 450 nm from the differential spectra of DT reduced minus CO-bound.[45]

AFM Sample Preparation. Gold substrates (Arrandee, Germany) consist of a vacuum evaporated thin gold film (thickness 200 nm) on borosilicate glass. They were annealed with a butane flame to obtain flat recrystallized Au(111) terraces. The annealed gold surface showed atomically flat (111) terraces over hundreds of nanometers. Before incubation of the BMP with gold substrates, the protein solution was treated for 1 h at 4 °C with 2 mM dithiotreitol (DTT) to reduce intermolecular disulfide bonds, thus eliminating protein dimers in solution. The excess DTT was removed immediately prior to immoblization experiments by gel filtration using a PD10 column (GE-Healthcare). At the same time, the storage buffer was exchanged to 100 mM potassium phosphate buffer pH 7.4.

The protein molecules were bound on Au(111) surface by directly incubating the freshly annealed gold substrates with 0.2 μM of protein solution (in 100 mM potassium phosphate buffer pH 7.4) for 30 min at +4 °C. The formation of the CST-MALM monolayer was formed by immersion of freshly annealed substrates into a 0.2 mM cystamine solution and incubated for 2 h. *N*-Succinimidyl 3-maleimidopropionate (1 mM in tetrahydrofuran) was allowed to react with the cystamine monolayer for 1 h at 4 °C. Samples were then rinsed with ultrapure water and blown dry with pure nitrogen. The maleimide terminated monolayer was then reacted with 0.2 μM of protein solution (in 100 mM potassium phosphate buffer pH 7.4) for 1 h at 4 °C. The samples were then rinsed with ultrapure water and immediately imaged by TMAFM.

The formation of the DTME monolayer was obtained by immersing freshly annealed substrates into a 2 mM DTME solution in dimethilsulfoxide (DMSO) overnight at room temperature. Samples were rinsed with DMSO and subsequently with ultrapure water and blown dry with pure nitrogen. The maleimide-terminated monolayer was then reacted with 0.2 μM of protein solution (in 100 mM potassium phosphate buffer pH 7.4) for 1 h at 4 °C. Samples were then rinsed with ultrapure water and immediately imaged by TMAFM.

Tapping Mode AFM Measurements. TMAFM measurements were performed with a Nanoscope IIIa/Multimode, Digital Instruments equipped with a 12-mm scanner operating in the tapping mode. Silicon probes (Digital Instruments), 100 or 200 mm long, with nominal radius of curvature less than about 20 nm and spring constants of 0.15 and 0.57 N/m, respectively, were used. All protein imaging was performed in ultrapure water (18.2 MΩ/cm) using the commercial fluid cell (Digital Instruments) without the O-ring seal. Resonance peaks in the frequency response of the cantilever were chosen in the range of 8−30 kHz. Free oscillation of the cantilever was set to have a root-mean-square amplitude corresponding to ~1.5 V; after engaging, the set point was adjusted during scans to minimize the force between the tip and the sample. The surface sample roughness (Rq) expressed as $(\Sigma z_i^2/n)^{1/2}$ was calculated by using an analysis option of the AFM software.

Electrochemical Measurements. A three-electrode cell setup was used for the electrochemical measurements with a silver/silver chloride and a platinum wire as the reference and counter electrodes, respectively. The gold working electrode was the same as the one used for AFM studies (Arrandee, Germany) and functionalized as reported in the previous section. Electrochemical experiments were carried out at room temperature (25 °C) and in 100 mM potassium phosphate buffer pH 7.4, containing 100 mM KCl. All measurements were carried out under anaerobic conditions in a glovebox. Cyclic voltammograms were recorded using an Autolab PGSTAT12 potentiostat (Ecochemie, The Netherlands) controlled by GPES3 software.

RESULTS AND DISCUSSION

Wild type BMP presents three cysteine residues: C62, C156, and C400. The latter cysteine is the heme ligand and therefore was omitted from mutagenesis. The solvent exposure analysis of C62 and C156 were made by using the 3D structure of the wild type BMP. The calculated average exposure values for C62 and C156 are 11.6 and 1.0 Å^2, respectively.

In order to generate proteins where only one single surface cysteine is present at any one time, mutants C62S and C156S were constructed. A double mutant C62S/C156S without any exposed cysteines was also generated to be used as a control.

UV−vis spectra of the purified proteins, wild type, C62S, C156S, and C62S/C156S, were taken and all showed the typical Soret peak at 418 nm, characteristic of the low spin iron, along with bands at 568 and 535 nm (data not shown). The Soret peak shifted to 450 nm upon reduction and bubbling with carbon monooxide which is consistent with the formation of the reduced heme−carbon monooxide adduct, characteristic of an active P450 enzyme.[8]

The purity of the protein was calculated from the A_{419}/A_{280} ratio. The values obtained are between 1.1 and 1.4 for all the proteins, in agreement with those obtained in literature for pure BMP.[6,7] The presence of dimeric protein was evaluated with native gel electrophoresis, in the presence and absence of a reducing agent. Although dimers were present in all protein samples (with the exception of the double mutant), less dimer was observed in the case of C62S. For uniformity of experimental procedure, all samples were treated with dithiothreitol as the reducing agent prior to immobilization to ensure full activity of the thiol groups.

(44) Li, H.; Darwish, K.; Poulos, L. T. *J. Biol. Chem.* **1991**, *266* (18), 11909–11914.
(45) Omura, T.; Sato, R. *J. Biol. Chem.* **1964**, *239*, 2379–2385.

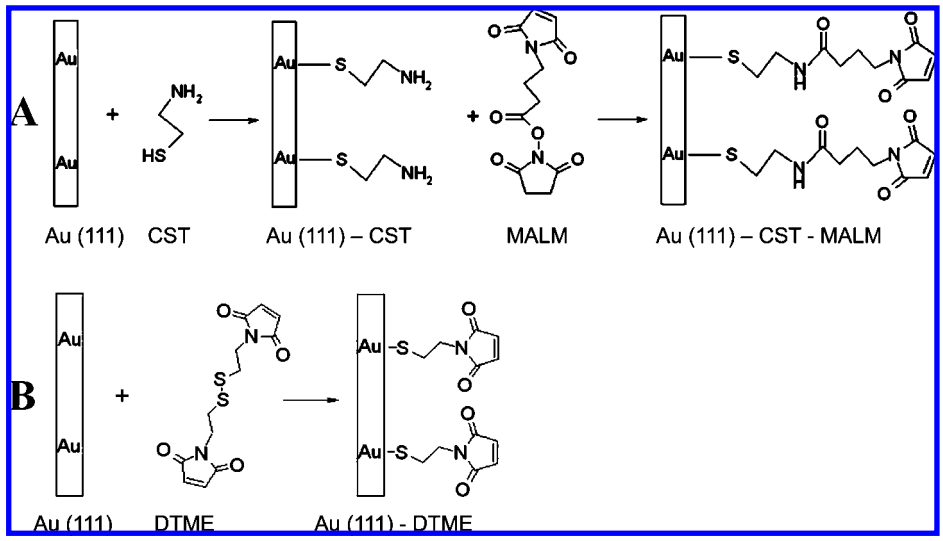

Figure 1. Schematic representation of strategies for the linkage of (A) cystamine-*N*-succinimidyl 3-maleimidopropionate (CST-MALM) and (B) dithio-bismaleimidoethane (DTME) spacers onto Au(111) surfaces.

Attachment of proteins to gold surfaces can be obtained by either direct covalent linkage of the SH group of the cysteine to the Au,[46,47] or via chemical spacers,[48,49] in all cases achieving a controlled orientation of the covalently linked protein.[49−53] In the latter situation, the reactivity of the spacer must be asymmetric so that one end reacts with the Au surface, while the other reacts with the protein's thiol.

The strategies used in this work are shown in Figure 1. The process shown in Figure 1A uses a two-step procedure, where cystamine binds to Au(111) via its thiol group generating an amine-terminated monolayer. This then reacts with the heterobifunctional linker *N*-succinimidyl 3-maleimidopropionate, able to form a stable amide linkage with the amine group of the cystamine. The latter presents a maleimido-group that primarily reacts with the thiol of the cysteine of the protein. On the other hand, in the strategy shown in Figure 1B, the DTME binds to the Au(111) surface via the thiol group deriving from the disulfide bond. Once the spacer is bound to the Au, the maleimido-group is freely accessible to react with the thiol of the cysteine. Both strategies lead to the covalent immobilization of the P450 enzymes on the modified gold substrate.

The morphology of wild type and mutants directly immobilized on Au(111) was characterized by TMAFM. Changes in incubation time and protein concentration were found to modulate the density of adsorbed molecules on Au(111). It was observed that protein concentrations of 1−2 μM incubated for 1 h at 4 °C led to samples difficult to image, due to the adsorption of too many molecules, probably forming multilayers. Optimal images of individual molecules at high resolution were obtained by using a protein concentration of 0.2 μM incubated for 1 h at 4 °C.

Representative topographic images of the proteins adsorbed directly on the Au(111) are shown in column 1 of Figure 2. The images of wild type and C156S show single molecules clearly visible on the Au(111) surface. These images are reproducible upon consecutive scans, thus indicating that these proteins are stably immobilized. The reproducibility of TMAFM images allowed the measurement of the heights of more than 100 single molecules as shown in column 4 of Figure 2. On the other hand, topographic images of C62S show the presence of both single molecules and aggregates that could be displaced by repeated scans. These observations indicate that the attachment of this mutant to the Au(111) surface is due to both covalent and noncovalent interactions. Topographic images of the C62S/C156S double mutant (data not shown) were not of appreciable quality due to large protein aggregates which were formed on the gold surface in the absence of any covalent interactions leading to fouling of the AFM tip. This is interpreted by the inability of this mutant to form covalent bonds due to the absence of any thiols.

The heights of the immobilized wild type and mutants were measured on the cross-section profiles of the individual molecules, as shown in Figure 2, columns 2 and 3. The result from the statistical analysis of over 100 molecules is shown in column 4 of Figure 2. In all samples a monomodal distribution is found. The mean height of the adsorbed protein molecules on the gold surface are 1.7 ± 0.4 nm for wild type, 2.0 ± 0.6 nm for C156S, and 2.5 ± 0.8 nm for C62S. Literature data show similar AFM molecular height values obtained for other P450 enzymes which were directly adsorbed on various solid supports such as mica and graphite.[54,55] However, these values are relatively low when compared to the calculations made from the protein structure.[6,7] In fact, taking into account the 3D structure of BMP and the different locations of C62 and C156 on the surface of the protein, the expected molecular height of the immobilized native C62S

(46) Hu, Y.; Das, A.; Hecht, M. H.; Scoles, G. *Langmuir* **2005**, *21*, 9103–9109.
(47) Quiocho, F. A. *Philos. Trans. R. Soc. London* **1990**, *326* (1236), 341–351.
(48) Lei, C.; Hu, S.-Q.; Gao, N.; Shen, G.-L.; Yu, R.-Q. *Bioelectrochemistry* **2004**, *65*, 33–39.
(49) Yang, W.; Wang, J.; Zhao, S.; Sun, Y.; Sun, C. *Bioelectrochemistry* **2006**, *69*, 158–163.
(50) Carmon, K. S.; Baltus, R. E.; Luck, L. A. *Anal. Biochem.* **2005**, *345*, 277–283.
(51) Luck, L. A.; Moravan, M. J.; Garland, J. E.; Salopek-Sondi, B.; Roy, D. *Biosens. Bioelectron.* **2003**, *19*, 249–259.
(52) Tripathi, A.; Wang, J.; Luck, L. A.; Suni, I. I. *Anal. Chem.* **2007**, *79*, 1266–1270.
(53) Baltus, R. E.; Carmon, K. S.; Luck, L. A. *Langmuir* **2007**, *23*, 3990–3995.
(54) Kuznetsov, V. Y.; Ivanov, Y. D.; Archakov, A. I. *Proteomics* **2004**, *4* (8), 2390–2396.
(55) Kiselyova, O. I.; Yaminsky, I. V.; Ivanov, Y. D.; Kanaeva, I. P.; Kuznestov, V. Y.; Archakov, A. I. *Arch. Biochem. Biophys.* **1999**, *371* (1), 1–7.

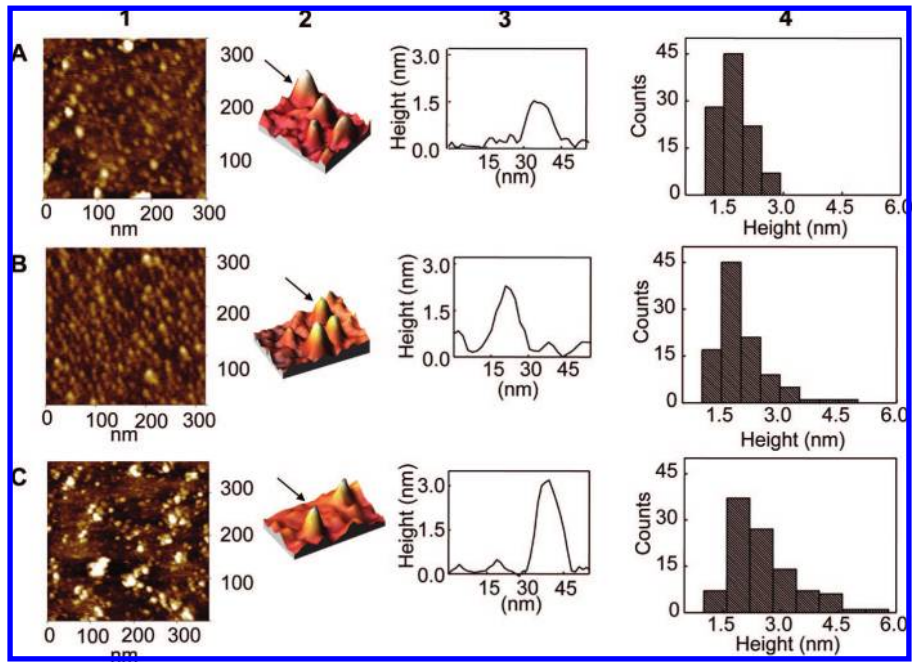

Figure 2. TMAFM of BMP wild type (A), C156S (B), and C62S (C) directly adsorbed on Au(111). Column 1: TMAFM two-dimensional images recorded in milli Q water, *z* range 8 nm. Column 2: three-dimensional view of single proteins (image size 50 nm × 75 nm, *z* range 3.5 nm). Column 3: cross-section of single protein profiles. Column 4: histograms of the molecular heights calculated from individual cross section profiles of >100 molecules, the mean height is 1.7 ± 0.4 nm for wild type, 2.0 ± 0.6 nm for C156S, and 2.5 ± 0.8 nm for C62S.

Table 1. Comparison of the Theoretical Heights Expected from the 3D Structure Analysis of BMP and Those Experimentally Determined by TMAFM Measurements on the Immobilized Proteins

	Remaining cysteine residue	Cys solvent exposure (Å^2)	theoret height from 3D structure (nm)	heights measured by TMAFM (nm)		
				direct immobilization on gold	CST-MALM spacer	DTME spacer
BMP-wt	C62 + C156	1.0−11.6	5−6	1.7 ± 0.4	5.5 ± 1.5	6.6 ± 1.6
BMP-C156S	C62	11.6	6	2.0 ± 0.6	6.0 ± 2.3	3.9 ± 1.4
BMP-C62S	C156	1.0	5	2.5 ± 0.8	4.7 ± 1.5	3.6 ± 0.9
BMP-C62S/C156S	none	0.0				

on bare gold (i.e., through the sulfur atom of C156) is about 5 nm, while that of C156S (i.e., through the sulfur atom of C62) is about 6 nm (Table 1).

The discrepancy between the theoretical and the experimentally determined values is explained in terms of extensive interactions of the proteins with the metal surface, responsible for conformational changes or even partial unfolding, as also found for other metalloproteins.[2,56] Although both the binding of wild type and single mutants to gold is expected to occur mainly through the free thiol group of the cysteine residue, the results observed here point to the presence of additional electrostatic interactions.[57] Regarding the lateral size of the proteins in the TMAFM images, these data are in general less informative, because of the relatively large size of the tip and its geometry induced broadening effects on the imaged biomolecules.[2,58]

On the basis of these findings, the gold surface was functionalized with spacers with the objective of shielding the protein from the strong interactions with the metal surface. The spacer is also expected to add some level of flexibility that is more compatible with the correct fold of the P450, while maintaining an ordered orientation through the selective reactivity to the cysteine thiol of the protein.

To this end, the formation of the CST-MALM monolayer was obtained by varying the concentrations of cystamine and *N*-succinimidyl 3-maleimidopropionate as well as the incubation time and temperature (data not shown). The best conditions for the formation of the monolayer were found to be 0.2 mM cystamine in water for 2 h at room temperature and 1 mM of *N*-succinimidyl 3-maleimidopropionate in tetrahydrofuran for 1 h at 4 °C. Column 1 of Figure 3A shows a TMAFM image in an aqueous solution of the CST-MALM monolayer assembled on the gold surface. The functionalized gold shows a surface roughness (Rq) of 0.46 ± 0.12 nm on 300 nm × 300 nm sample areas, which is considerably higher when compared to the value of 0.15 ± 0.10 nm observed for the bare Au(111) surface.

The immobilization of both wild type and C156S on the CST-MALM functionalized Au(111) gave rise to a significant increment in surface roughness (1.52 ± 0.19 and 1.37 ± 0.11 nm, respectively), with the appearance of globular shaped structures identified as

(56) Davis, J. J.; Hill, H. A. O. *Chem. Commun.* **2002**, *5*, 393–401.
(57) Venkataraman, L.; Klare, J. E.; Tam, I. W.; Nuckolls, C.; Hybertsen, M. S.; Steigerwald, M. L. *Nano Lett.* **2006**, *6* (3), 458–462.
(58) Markiewicz, P.; Goh, M. C. *J. Vac. Sci. Technol.* **1995**, *13* (3), 1115–1118.

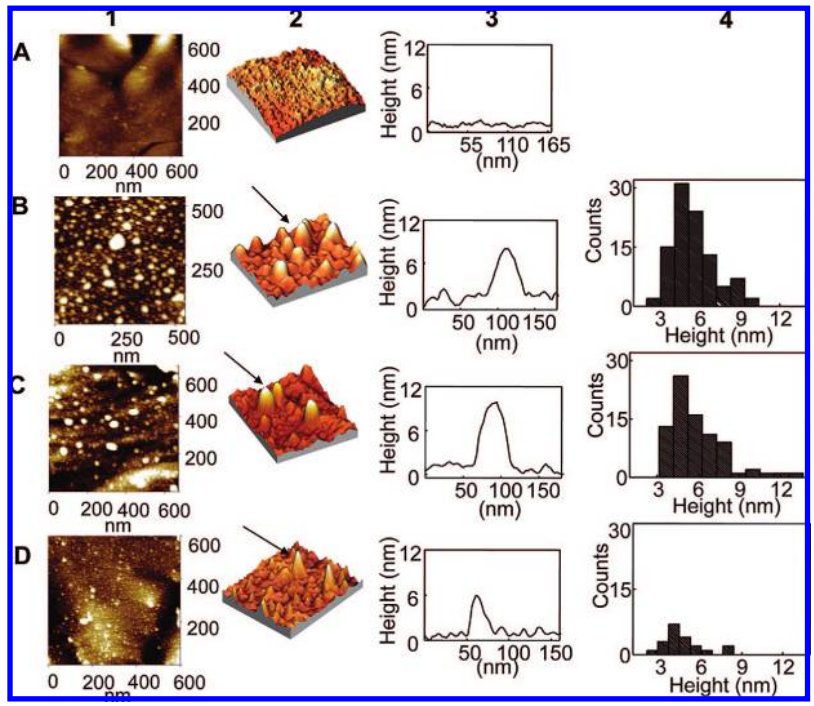

Figure 3. TMAFM of CST-MALM bound to Au(111) before (A) and after the linkage of wild type (B), C156S (C) and C62S (D). Column 1: TMAFM two-dimensional images recorded in milli Q water, *z* range 8 nm. Column 2: three-dimensional view of single proteins (image size 180 nm × 250 nm, *z* range 12 nm). Column 3: cross-section of single protein profiles. Column 4: histograms of the molecular heights calculated from individual cross section profiles of >100 molecules (except for C62S where around 23 molecules were considered); the mean height is 5.5 ± 1.5 nm for wild type, 6.0 ± 2.3 nm for C156S, and 4.7 ± 1.5 nm for C62S.

single protein molecules as shown in Figure 3B,C (column 1). The number of molecules assembled on the surface for the wild type is slightly higher than that obtained for the C156S. This difference is much more evident for the C62S, where the sample roughness (0.70 ± 0.17 nm) is only slightly higher with respect to the CST-MALM monolayer alone, and the number of protein molecules assembled on the modified gold is considerably lower than that observed for wild type and C156S mutant (Figure 3D, column 1 and 2). Wild type and single mutants allowed to measure stable TMAFM images reproducible after repetitive scans: the single molecules were well resolved with no evidence of protein mobility on the substrate surface. This is typical of a stable binding of proteins to the modified Au(111) substrate. On the other hand, the C62S/C156S double mutant did not lead to images of appreciable quality (data not shown): in this case the absence of cysteines did not allow the binding of the protein to the thiol-specific spacer. Moreover, the presence of the spacer on the gold surface decreases the ability of noncovalent interactions between the protein and the surface lowering the physisorption that was hypothesized for the bare gold.

The height of proteins in the images was evaluated by cross section analysis on single molecules (column 3 of Figure 3), excluding contributions of the background roughness. The obtained heights are plotted in the histograms of column 4 in Figure 3. The mean height values are 5.5 ± 1.5 nm for wild type, 6.0 ± 2.3 nm for C156S, and 4.7 ± 1.5 nm for C62S; it has to be mentioned that the statistical analysis for the C62S mutant was obtained only considering a few molecules (on average between 20−35), due to the lower yield of immobilization.

Here the values of protein heights are in excellent agreement with the expected molecular dimensions for the two different protein orientations on functionalized Au(111) derived from the linkage of the different cysteine residues (see Table 1). Moreover, C62 has a calculated surface accessible area of 11.6 Å^2, and this is expected to facilitate the reaction with the maleimide group for both the wild type and the C156S mutant. These observations confirm that C62 is indeed the preferred anchoring group. Therefore, the linkage obtained for the C156S mutant via C62 allows the immobilization of many protein molecules on the maleimide-modified surface. On the other hand, the low accessibility of C156 (1.0 Å^2) could explain the lower reactivity seen with the maleimide linker (also consistent with less dimer observed for this mutant, as mentioned earlier).

The functionalization of the gold substrate was also achieved by using DTME. The use of this linker offers the combined advantage of a shorter carbon chain, hence decreasing the distance between the protein and the gold, and a simpler chemistry involving only one reaction step.

The linkage of DTME to gold was obtained by varying the protein concentration as well as the incubation times and temperatures (data not shown). The best conditions for a monolayer formation were found to be overnight incubation with 2 mM of DTME at room temperature.

Figure 4A (column 1) shows a typical TMAFM image acquired on Au(111) derivatized with DTME. The sample has a surface roughness of 0.38 ± 0.10 nm on a 300 nm × 300 nm sample area, a value lower than that obtained for the CST-MALM monolayer.

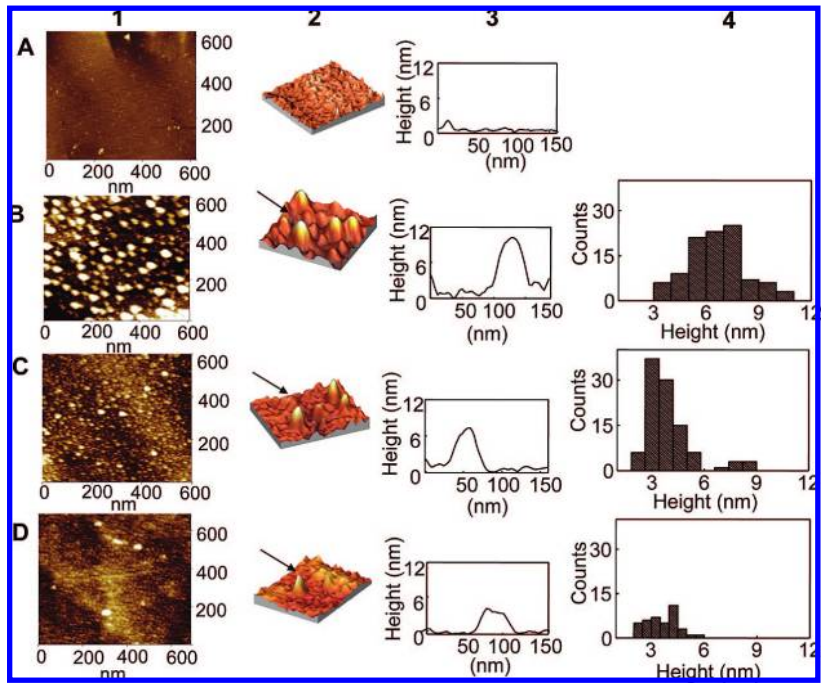

Figure 4. TMAFM of DTME bound to Au(111) before (A) and after the linkage of wild type (B), C156S (C), and C62S (D). Column 1: TMAFM two-dimensional images recorded in milli Q water, *z* range 8 nm. Column 2: three-dimensional view of single proteins (image size 180 nm × 200 nm, *z* range 12 nm). Column 3: cross-section of single protein profiles. Column 4: histograms of the molecular heights calculated from individual cross section profiles of >100 molecules (except for C62S where around 30 molecules were considered); the mean height is 6.6 ± 1.6 nm for wild type, 3.9 ± 1.4 nm for C156S, and 3.6 ± 0.9 nm for C62S.

Figure 4B−D (columns 1 and 2) shows that following exposure of the modified gold surface to wild type and mutants of BMP, single structures with globular shape appear on the surface. These TMAFM images are stable and reproducible after repetitive scans, and individual proteins are well resolved with no evidence of mobility on the substrate surface. This is typical for a strong binding of proteins to the modified Au(111). A significant increase of surface roughness (1.89 ± 0.46 nm) is observed for the wild type, while moderate increments for the C156S (0.73 ± 0.14 nm) and the C62S (0.53 ± 0.09 nm) mutants are observed. These variations in roughness are a consequence of the different number of protein molecules immobilized. The C62S/C156S double mutant again did not lead to images of appreciable quality or interpretation (data not shown), confirming that exposed cysteine residues are required for the immobilization with the spacer.

The histograms of protein heights on DTME, as measured from single-molecule cross-section profiles, are shown on column 4 of Figure 4. The distributions are centered at mean height values of 6.6 ± 1.6 nm for wild type, 3.9 ± 1.4 nm for C156S, and 3.6 ± 0.9 nm for the C62S.

The heights measured by TMAFM for the wild type and C62S and the lack of binding of the double mutant to the DTME spacer are in line with the results obtained for the CST-MALM. However, the height data measured for the C156S mutant, which was predicted to behave like the wild type, gave a lower than expected height of 3.9 nm. This value is in between that of denatured BMP on bare gold (around 2 nm) and native protein (around 5−6 nm). This can be explained by a nonhomogeneous distribution of DTME on Au(111) that leaves patches of bare gold that adversely interact with the protein causing partial denaturation.

When the electrochemical performance of the immobilized proteins was tested, no measurable response was observed when any of the proteins were directly adsorbed on gold. Henceforth only the data with functionalized gold substrate will be discussed. Moreover, neither the C62S nor the double mutant showed any detectable electrochemistry with the functionalized gold electrodes.

Typical cyclic voltammograms recorded for wild type and C156S under anaerobic conditions on gold modified with CST-MALM in phosphate buffer, pH 7.4, are shown in Figure 5A. As can be observed, modification with CST-MALM gave rise to two waves with a midpoint potential of −48 ± 10 and −58 ± 8 mV (vs NHE) for the wild type and C156S, respectively. These values are in agreement with values previously reported for this protein and other P450s on different electrodes.[17,11,28] The peak current for both proteins is linear with scan rates up to 100 mV indicating that it is immobilized on the gold electrode surface. The peak-to-peak separation did not vary within the range considered, but in all cases a larger than the normal value of 59 mV was observed for the redox couple. This can be attributed to slow electron transfer rates of these proteins while immobilized on gold electrodes, a phenomenon also seen with other P450s.[28] Calculation of electron transfer rates using Laviron's approach[59] was prevented due to instrument limitations because scanning at higher scan rates was not possible.

With regards to the electrochemical behavior of these two proteins immobilized on gold electrodes functionalized by DTME, similar data to those of CST-MALM were obtained as shown in Figure 5B. In this case the observed waves had a midpoint potential of −89 ± 8 and −49 ± 5 mV (vs NHE) for wild type and

(59) Laviron, E. *J. Electroanal. Chem.* **1979**, *101*, 19–28.

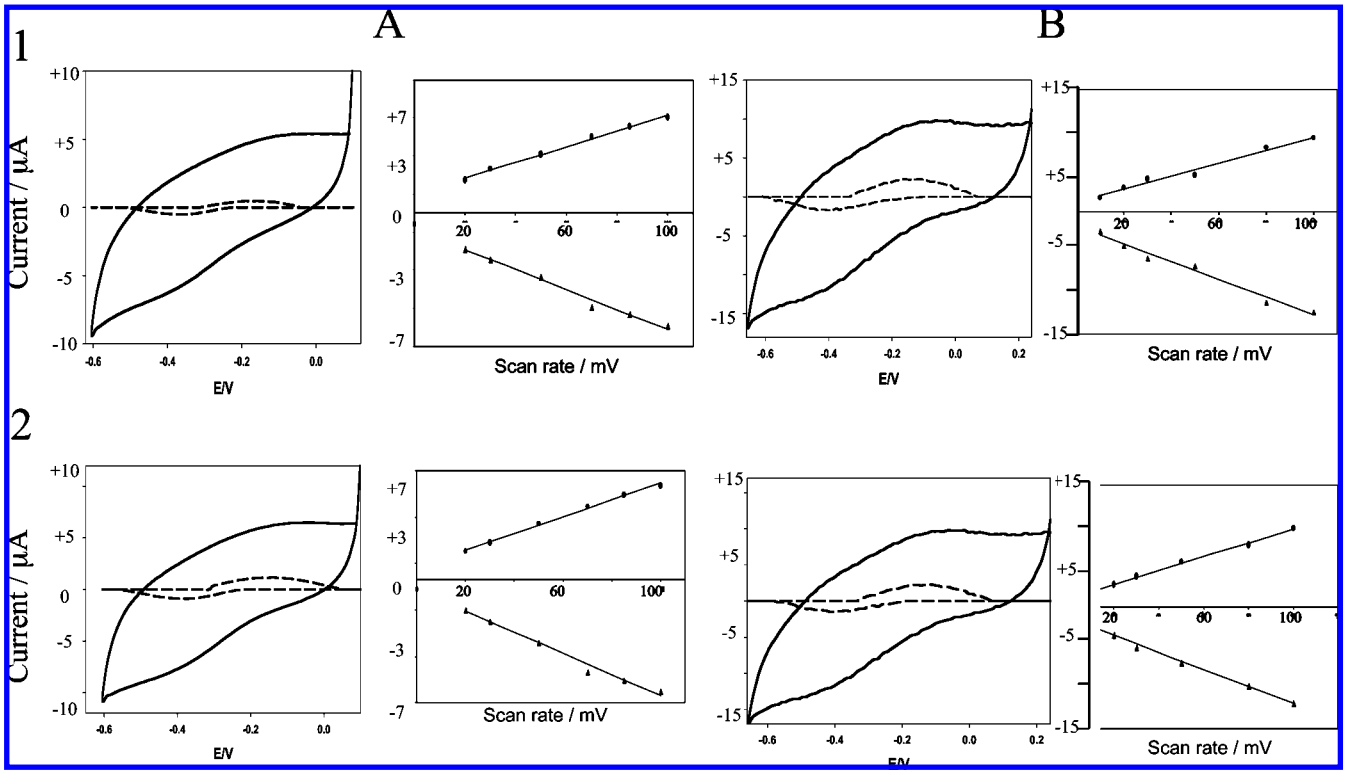

Figure 5. Cyclic voltammograms of wild type (1) and C156S mutant (2) on Au electrodes modified with CST-MALM (A) and DTME (B). Scan rate 100 mV s^{-1} in 100 mM potassium phosphate with 100 mM KCl pH 7.4. The original voltammograms (solid lines) are shown together with the baseline corrected ones (dotted lines). The corresponding dependence of peak current on the scan rate is also shown for each protein and linker combination.

C156S, respectively. The peak current for both wild type and C156S is linear with scan rates up to 100 mV indicating that the proteins are immobilized on the gold electrode as was seen with CST-MALM modification. Again there is a larger than expected peak-to-peak separation which can be attributed to slow electron transfer rates, as discussed previously.

Comparison of the midpoint potentials values of all proteins on the different spacers again shows an anomaly for the DTME-derivatized gold. This result is in line with the TMAFM data where a nonhomogeneous distribution of the DTME on Au(111) was inferred.

CONCLUSIONS

TMAFM images of wild type and mutant cytochrome P450 BMP were successfully visualized down to the resolution of single proteins. All data are summarized in Table 1. In all cases, binding to bare gold led to molecular heights lower than those expected from crystallographic data and the absence of electrochemical signals confirms the presence of adverse interactions between the metal surface and the proteins causing unfolding.

On the other hand, molecular heights compatible with the predictions made on the basis of the protein structures were obtained using CST-MALM and DTME. The analysis of these images indicates that the different solvent exposure of the cysteines strongly affects the binding efficiency to the derivatized gold substrate. In fact the wild type protein and C156S mutant exhibit a strong tendency to bind to both the CST-MALM and DTME spacers leading to good yields of immobilization. This is consistent with the higher solvent accessibility of the C62 residue present in both proteins.

For both spacers it was observed that the C62S mutant, bearing the lowest exposed C156 cysteine, exhibits a lower tendency to binding to the functionalized gold surface. The C62S/C156S double mutant did not lead to stably immobilized proteins, confirming the necessity of cysteine residues to lead to a covalent linkage.

Comparison of the results obtained from the CST-MALM and DTME spacers show some unexpected results for the latter linker, and these are interpreted in terms of lack of homogeneity of the surface due to inefficient binding of the linker to the gold leading to patches of bare gold where the protein tends to flatten, resulting in the variability seen in the height measurements (Table 1). Although the DTME strategy was theoretically the preferred one, due to its simple one step reaction and shorter electron transfer distance between the protein and the electrode, problems were observed concerning its ability to form homogeneous and ordered monolayer on gold, leading to an aspecific binding of the proteins.

These data are confirmed by electrochemistry where the wild type and the C156S mutant gave a measurable electrochemical signal when immobilized using the CST-MALM and DTME spacers. The C62S and the double mutant did not give any appreciable current in both cases. The electrochemical results also confirm the findings of the TMAFM, whereby the C62 is the preferred point of covalent linkage to the derivatized gold and that the presence of a spacer is key to obtaining an electrochemically active BMP on gold electrodes.

In summary, the data presented in this paper prove there are two crucial levels of engineering in order to achieve an electrochemically active P450 electrode. At the protein level, it is important for the presence of a highly exposed unique cysteine residue capable of covalent linkage

to the surface. On the electrode surface, it is crucial to introduce a spacer that binds to the gold forming a homogeneous layer, while at the same time allowing flexibility to the protein. This is important to maintain an active and folded protein structure. The approach followed in this paper should also leave the channel to the active site exposed toward the bulk environment necessary to maintain activity.

ACKNOWLEDGMENT

G. Gilardi acknowledges support from the EU Marie Curie Project EdRox-MRTN-035649 and the Regione Piemonte (IT). L. Andolfi acknowledges the MIUR project "Rientro dei cervelli". The work was also partially supported by PRIN-MIUR 2006 (Grants 2006028219 and 2006027587).

Received for review June 5, 2008. Accepted September 18, 2008.

AC8011413